

# Investigation of correlation effects in FeSe superconductor by LDA+U method

H. Lohani, P. Mishra and B. R. Sekhar

October 31, 2023

## Abstract

Correlation effects are observed strong in Iron chalcogenides superconductors by experimental and theoretical investigations. We present a comparative study of the influence of Coulomb interaction and Hund's coupling in the electronic structure of FeSe and FeTe. The calculation is based on density functional theory (DFT) with local density approximation(LDA+U) framework employed in TB-LMTO ASA code. We found the correlation effects were orbital selective due to the strength of interorbital hybridization among different Fe-3d orbitals mediated via chalcogen (Se/Te-p) orbitals is different in both the compounds, however Coulomb interaction is screened significantly by Te-p bands in FeTe. Similarly the orbital section is different in both the compounds because of the difference in the chalcogen height.

## 1 Introduction

Iron based superconductors, particularly members of  $\text{FeSe}_{1-x}\text{Te}_x$  family attract much attention due to their nature of strong electron correlation unlike other superconductors. A recent advancement in this field is the synthesis of single-layer films of FeSe on  $\text{SrTiO}_3$  substrates exhibiting superconductivity ( $T_c=80$  K) which turns insulating with the addition of one more layer[1]. This unusual behavioral difference between single and double layer films of FeSe is a signature of strong electron correlation which has been experimentally observed[2, 3]. Superconductivity in the  $\text{FeSe}_{1-x}\text{Te}_x$  compounds was first reported by Hsu *et al.* [4] in the FeSe ( $x = 0$ ) compound exhibiting a  $T_c$  around 8 K which rises up to 37 K under pressure (7GPa)[5]. On the other hand, the other extreme composition of this family,  $\text{Fe}_{1.068}\text{Te}$ , though not a superconductor show a spin density wave (SDW) ordering at 67K[12] with an accompanying structural transition from tetragonal to monoclinic. With Se doping superconductivity emerges in FeTe with a simultaneous decrease in the SDW and the value of  $T_c$  reaches maximum 15 K for  $x = 0.5$  doped case. The Fe content is also detrimental for superconductivity; with excess Fe favors the spin localization destroying the superconductivity[14, 15]. Both FeSe and FeTe have tetragonal crystal structure belonging to space group symmetry  $P_4/nmm$ . It consists a square planar sheet of Fe atoms, which is tetrahedrally coordinated with anion (Se/Te) atoms. However, the height of anion atom from the Fe square plane is different in these two compounds and this plays a pivotal role in determining the electronic properties of these systems[10, 13].

A recent ARPES study on  $\text{FeSe}_{1-x}\text{Te}_x$  compositions by Ieki *et al.* [39] has shown clearly the strong electronic correlation in these compounds, where a small quasi particle weight in FeTe transforms into a sharp one with increase in Se content. Other ARPES results [32, 37] on these compounds have shown significant band renormalization which was supported by the calculations based on local density approximation (LDA). Tamai *et al.* [35] has found the mass renormalization factor to be  $m^*/m = 20$  from their ARPES study on  $\text{FeSe}_{0.42}\text{Te}_{0.58}$ . It is close to the value observed in highly correlated systems like transition metal oxides. Also, our angle integrated valence band photoemission study on  $\text{FeSe}_{1-x}\text{Te}_x$  [19] revealed significant spectral weight shifts in the near  $E_f$  region with Se doping leading to the formation of a pseudogap. Further, a temperature dependent orbital selective spectral weight transfer was also reported by us[19]. Although, such manifestations of the strong coulomb correlation were also shown in many other photoemission studies[20, 36], these experimental observations are not well addressed by LDA based electronic structure calculations. However, results of some recent calculations[17, 18, 31], where Coulomb correlations were included by using LDA+DMFT frame work, are very close to the experimental findings. In this paper we are presenting our calculations showing the evolution of electronic structure by the incorporation of different values of Coulomb interaction  $U$  and intra-atomic exchange  $J$  based on LDA+U scheme in FeSe and FeTe. We observed multi

orbital correlation effect in Fe-3d states which is more prominent in FeSe in comparison to FeTe. We have discussed our results referring to the difference in the geometry of the anion tetrahedra in both the compounds.

## 2 Details of Calculation

The band structure calculations we performed were based on first principles Langreth-Meh-Hu gradient corrected von Barth Hedin parametrized LDA [27] energy and potential. Lattice parameters used in the calculations are taken from the experimental data[21, 22] published earlier by others. Correlation effects of the Fe-3d orbitals have been examined by employing different values of Coulomb interaction parameter  $U$  and Hund's coupling  $J$ [28]. Empty spheres were introduced to make the volume of the unit cell equal to the total volume of the spheres within the permissible limit of atomic sphere approximation (ASA). Fe-4s, 4p, 3d ; Se-4s, 4p, 4d and Te-5s, 5p, 5d orbitals are used as the basis set for the valence energy region. A mesh of  $12 \times 12 \times 8$  is used for sampling the irreducible part of the Brillouin zone integration. Height of the anion atom from the Fe square plane was relaxed by minimizing the total energy using Quantum Espresso code[29]. We checked our calculation parameters by comparing them with the LDA results reported earlier[36, 30].

## 3 Results and Discussion

### 3.1 DOS

Fig (1a) and (1b) show the plots of density of states (DOS) for FeSe and FeTe respectively for the range of 4.0 to -7.0 eV binding energy (BE). The valence band (VB) DOS comprises of the region from  $E_f$  to -6.0 eV BE while the unoccupied DOS extends from  $E_f$  to 3.0 eV BE. The near  $E_f$  states from 2.8 to -2.4 eV are predominantly Fe-3d derived for both FeSe and FeTe. These Fe-3d states, separated in lower and upper bands exhibit a clear pseudogap feature just above the  $E_f$  (0.24 eV) in the case of FeSe whereas it is less prominent in the case of FeTe. The states around -2.2 to -6.0 eV are originate from the Fe-3d and anion (Se/Te)-p hybridized states. Interestingly, for the case of FeSe, there exists a sharp gap at -2.3 eV which is not present in case of FeTe. Due to the smaller electronegativity of Te compared to Se, the hybridized states between Fe-3d and anion-p orbitals are placed at a lower BE in FeTe in comparison to those of FeSe. DOS have also been calculated after downfolding the valence orbital of the anion atom (Fig (1c) and (1d)) in order to get a deeper insight into the role of anion orbitals. The gap at -2.3 eV present in Fig (1a) is due to the splitting of bonding and antibonding bands between Fe-3d and Se-p hybridized states which becomes less prominent when the valence orbitals of Se atom are downfolded as shown in Fig (1d). Similarly the pseudogap feature across the  $E_f$  is also associated with the hybridization between Fe-3d and Se-p orbitals. Unlike FeSe, the anion orbitals do not play any major role in modifying the DOS in FeTe as is clear from Fig (1b) and (1d). It indicates a weak hybridization between Fe-3d and Te-p orbitals in FeTe. The role of the anion orbitals is linked to the structural geometry of FeSe and FeTe. The insets of Fig (1c) and (1d) show the geometry of anion tetrahedra in FeSe and FeTe respectively. This tetrahedral geometry depends on two important parameters; firstly, the height of anion from the Fe square plane ( $z$ ) which is 1.64 Å and 1.46 Å in case of FeTe and FeSe respectively and secondly, the anion-Fe-anion angle ( $\alpha$ ). The enhanced  $z$  height in case of FeTe reduces the interorbital hopping among the Fe-3d orbitals, mediated via anion p orbitals. Similarly, the value of  $\alpha$  is  $99.9^\circ$  in case of FeTe which increases to the perfect tetrahedron value  $109.4^\circ$  in case of FeSe. The large value of  $\alpha$  and small value of anion height ( $z$ ) makes a stronger hybridization between the Fe-3d and anion-p orbitals in case of FeSe in comparison to FeTe. This difference in hybridization strength is reflected in the plot of DOS Fig (1a) and Fig (1c).

Coulomb correlation effects are important in bands of narrow width, especially in Fe-3d states. So the changes in Fe-3d states under the influence of different values of  $U$  have been calculated and shown for FeSe and FeTe respectively in Panel (a) and (b) of Fig 2. In FeSe, Fe-3d states start localizing with the application of  $U$  and noticeable changes occur at higher values of  $U$ . For  $U = 4.0$  eV case, the pseudogap feature disappears around  $E_f$  and only two peaks are observed in the VB compared to the case of  $U = 0.0$  eV. These two peaks merge and shift towards higher BE with  $U = 5.0$  eV. In case of FeTe, the Fe-3d states also become localized under the application of  $U$ . However the amount of shift towards higher BE at large values of  $U$  (3.5 and 5.0 eV) is less and states are more at the vicinity of  $E_f$  at smaller values of  $U$  (1.0 and 2.0 eV). In addition to this, narrowing of the lower and upper bands of Fe-3d states with increase of  $U$  is less. It indicates that the effect of Coulomb correlation is weak in FeTe. Possible reason for this, is the presence of Te-p states at lower BE which screen the  $U$  strongly [23]. On the basis of previous reports [23, 17, 31] the value of  $U=4.0$  and 3.5 eV are chosen to see the evolution of Fe-3d states under the influence of  $J$  in FeSe and FeTe as shown in Fig 3(a) and 3(b) respectively. It is observed that the Fe-3d states are modified significantly even by introduction of a small value of  $J=0.1$  eV in case of FeSe. The Hund's coupling, shifts all the Fe-3d states towards

lower BE, with a simultaneous appearance of pseudogap slightly above  $E_f$ . With increase in the value of J further, there is no substantial changes in the DOS. In the case of FeTe, the Fe-3d states are also shifted towards lower BE, particularly the states near  $E_f$  increase gradually, with the incorporation of J though the changes are less as compared to FeSe. These results show that Hund's coupling J is a key factor in the formation of Fe-3d DOS.

In order to highlight the correlation effects, DOS of different Fe-3d orbitals are plotted at different values of U and J in FeSe and FeTe as shown in Panel (a) and (b) of Fig 4 respectively. In FeSe, in the absence of U and J, near  $E_f$  states and pseudogap feature arises from  $d_{yz/xz}$  and  $d_{x^2-y^2}$  orbitals. The states originating from  $d_{xy}$  orbital have largest splitting with two peaks at -1.7 and 1.6 eV BE in the DOS. Additionally, a clear gap is observed in  $d_{3z^2-r^2}$  states around  $E_f$  which are quite localized at -0.8 eV. Application of Coulomb interaction (U=4.0 eV), results in localization of the states derived from all four orbitals and the states shift towards higher BE. This shift is the largest in the states of  $d_{x^2-y^2}$  orbital. Major effect of U is observed in  $d_{yz/xz}$  states, where broad states near  $E_f$  transforms into two clear peaks at higher BE. Hence the pseudogap feature vanishes across  $E_f$ . Application of a small value of Hund's coupling J=0.1 eV, restore the  $d_{yz/xz}$  states near  $E_f$  and no significant changes are seen by further increasing the J value from 0.1 to 1.2 eV. This nature of pseudogap, which occurs in full range of Hund's coupling but absent when J=0.0 at U=4.0 eV, is consistent with the previous work of Ansgar *et al.* [18] where this pseudogap is attributed to a resonance in self energy caused by spin fluctuations. In case of FeTe in the absence of U and J values, near  $E_f$  states and pseudogap are also formed by  $d_{yz/xz}$  and  $d_{x^2-y^2}$  states like FeSe but a gap is present at -0.7 eV in  $d_{yz/xz}$  states as well as number of these states are more across the  $E_f$ . The  $d_{3z^2-r^2}$  and  $d_{x^2-y^2}$  states shift towards higher BE by switching on the U=3.5 eV and the amount of shift is quite small in comparison to FeSe. These states shows an incremental shift towards  $E_f$  with increase the J value in this case. These changes in DOS are presented in table 1, where the occupancy of electrons in different orbitals of Fe-d is tabulated, for quantitative analysis. The occupancy of  $d_{yz/xz}$  and  $d_{x^2-y^2}$  orbitals show an opposite behaviour for FeSe and FeTe under the influence of Coulomb correlation energy. On the other hand, a remarkable enhancement is observed in the occupancy of  $d_{x^2-y^2}$  orbital after introducing j= 0.1 eV in FeSe. It is almost twice in comparison to J=0.0 eV case. The change in the occupancy of Fe-3d orbitals due to the effect of U and J presented here summaries the orbital selective effect in Fe-3d orbitals in FeSe and FeTe. The individual occupancy of four orbitals are different which are further enhanced by Coulomb interaction and Hund's coupling. It turns out to a orbital selective nature of the correlation effect which is crucially depends on individual band filling factor[43].

## 3.2 Band

Fig 5 shows the near  $E_f$  band structure of FeSe with U = 0.0 (5a), U = 4.0 eV (5b) and FeTe with U = 0.0 (5c) and U = 3.5 eV (5d). Initially when U and J = 0.0 eV, three hole like and two electron like bands are observed at  $\Gamma$  and M point respectively in both FeSe and FeTe. However, the outer hole like bands are quasidegenerate in case of FeSe. In order to show the contribution of different Fe-3d orbitals, the fat bands are calculated for both FeSe and FeTe. These bands are plotted in Fig 5(e-h) for the FeSe case with U and J = 0.0 eV. Fatness of bands indicate that the innermost hole like band has a  $d_{yz/xz}$  and the outer two have  $d_{xy}$  and  $d_{x^2-y^2}$  orbital characters in both the compounds. Similarly the electron like bands are composed mainly of  $d_{x^2-y^2}$  with little contribution from the  $d_{yz/xz}$  orbital in FeSe while inner electron like band (-0.23 eV) has  $d_{yz/xz}$  and outer one (-0.47 eV) has  $d_{x^2-y^2}$  orbital character in FeTe. Another major difference is that the Te-p bands are intermixed with Fe-d bands opposite to that of FeSe, where Fe-d bands are quite separated from the Se-p bands. These Te-p bands screen the effect of Coulomb interaction U in FeTe, hence the value of U is smaller in FeTe in comparison to FeSe. After applying Coulomb interaction degeneracy of the  $d_{xy}$  and  $d_{x^2-y^2}$  hole like bands at the  $\Gamma$  point has been lifted as shown in Fig(5b). The  $d_{x^2-y^2}$  band moves towards lower BE and other two  $d_{xy}$  and  $d_{yz/xz}$  band move towards higher BE at  $\Gamma$  point. The same band moves in opposite direction in case of FeTe by the application of U= 3.5 eV. On the other hand, the separation between the two electron like bands at the M point is enhanced in FeTe unlike the FeSe case where both the electron like bands are quasidegenerate and shift towards the lower BE under the influence of U = 4.0 eV.

Evolution of the near Fermi bands in FeSe and FeTe, with the tuning of different values of J, are shown in panel a and b of Fig 6 respectively. In FeSe, at  $\Gamma$  point, The  $d_{x^2-y^2}$  band which was crossing the  $E_f$  comes down below the  $E_f$  and the  $d_{yz/xz}$  band which was not crossing  $E_f$ , crosses  $E_f$  after applying J = 0.1 eV. Similarly, degeneracy of the two electron like bands at M point is also lifted. In FeTe, a gradual shifting is observed in the hole like  $d_{x^2-y^2}$  band at the  $\Gamma$  point towards the  $E_f$  and a gradual decrease in the separation between two electron like bands at the M point under the influence of Hund's coupling.

In a recent ARPES report on FeSe two hole like bands have been observed around the  $\Gamma$  point and two bands, one electron like and the other hole like, at the M point from 40 meV below  $E_f$  [16]. Another ARPES study on  $\text{FeTe}_{1-x}\text{Se}_x$  for x=0, 0.2, 0.3, 0.4 and 0.45 compounds by Ieki *et al.* [39] reported three clear hole like bands at the  $\Gamma$  point ( $\alpha$ ,  $\alpha'$  and  $\beta$ ) which evolve with Se doping and a shallow electron pocket at the M point for x = 0.45. The  $\alpha'$

and  $\beta$  crosses  $E_f$  whereas  $\alpha$  is around 20 meV below  $E_f$ . Similar results have also been experimentally observed in  $\text{Fe}_{1.04}\text{Te}_{0.66}\text{Se}_{0.34}$  [37],  $\text{FeSe}_{0.42}\text{Te}_{0.58}$  [35],  $\text{Fe}_{1.03}\text{Te}_{0.7}\text{Se}_{0.3}$  [42] and  $\text{FeTe}_{0.55}\text{Se}_{0.45}$  [40]. On the other hand in  $\text{Fe}_{1.02}\text{Te}$  [48] and  $\text{Fe}_{1-x}\text{Te/Se}$  [32] only two hole like bands are observed at  $\Gamma$  point. The band renormalization factor also varies highly at different points of Brillouin zone. For example, in case of  $\text{FeSe}_{0.42}\text{Te}_{0.58}$  Tamai *et al.* [35] observed  $m^*/m=20$  for electron like band at the M point whereas it is just 6 for one of the hole like band at the  $\Gamma$  point. It is clear from Fig (5a) and (5c) that initially when U and J are not incorporated all the three hole like bands cross the  $E_f$  in both the compounds as well as electron like band is placed at higher BE (-0.29 eV) in FeSe and (-0.23 and -0.47 eV) in FeTe at the M point. Only when correlation effect is taken into account, one of the hole like bands comes down below the  $E_f$  and other two cross the  $E_f$  as well as electron like band approaches towards  $E_f$  as clear from Fig 6 where in case of FeTe at  $U = 3.5$  and  $J = 0.8$  eV, innermost hole like band appears at 0.18 eV below  $E_f$  at the  $\Gamma$  point and electron like band position is closer to  $E_f$  by 0.1 eV in comparison to  $U$  and  $J = 0.0$  eV case. This trend qualitatively matches with above mentioned experimental findings, although there is a difference in the absolute energy scale. The orbital character of these near  $E_f$  bands, revealed by photoemission studies using polarized light source, [37, 40] also agree with our results. These results signify the importance of electronic correlation in these compounds however further calculation is required to handle the correlation effects in a better way to bring down the difference between the experimental findings and calculated results based on LDA+U scheme.

From the transfer integral values, calculated by Miyake *et al.* for FeSe and FeTe [23], it is clear that this value is large between  $d_{xy}$  and nearest neighbour (nn)  $d_{3z^2-r^2}$  orbital. It builds a strong interorbital hybridization between  $d_{xy}$  and  $d_{3z^2-r^2}$  orbitals which leads to a localization of  $d_{3z^2-r^2}$  states at higher BE with a clear gap from  $E_f$ . The  $d_{xy}$  orbitals point towards the nn Fe site so it has a largest band width and shows two well separated peaks one in the valence band and the other in the conduction band. On the other hand, transfer integrals between  $d_{xy}$  and nn  $d_{x^2-y^2}$  orbital is small but for second nn it depends on the height of anion. It is large in case of FeSe in comparison to FeTe. Thus chalcogen-p enhances the interorbital hybridization between  $d_{xy}$  and  $d_{x^2-y^2}$  orbital which reflects in a prominent pseudogap structure in  $d_{x^2-y^2}$  states in FeSe. Moreover, interorbital hybridization between  $d_{xy}$  and second nn  $d_{yz/xz}$  orbital is also mediated via anion-p orbital, hence it is also large in case of FeSe and contributes to pseudogap feature. On the contrary, larger height of Te anion allows a finite value of transfer integrals between  $d_{yz/xz}$  with nn  $d_{3z^2-r^2}$  and  $d_{x^2-y^2}$  orbitals by breaking the mirror plane symmetry in case of FeTe. These inter orbital hybridizations are responsible for the gap in  $d_{yz/xz}$  states at -0.8 eV, which is absent in FeSe (Fig(4)). When Coulomb interaction is introduced, it reduces the interorbital hopping and mainly  $d_{yz/xz}$  and  $d_{x^2-y^2}$  states are affected which have large number of states near  $E_f$ . As a consequence of this, the electron is transferred from the in-plane  $d_{x^2-y^2}$  and  $d_{xy}$  to the out of plane  $d_{yz/xz}$  and  $d_{3z^2-r^2}$  orbitals and localized them at higher BE in case of FeSe. In FeTe, the transfer occurs from  $d_{xy}$  and  $d_{yz/xz}$  to  $d_{x^2-y^2}$  orbitals as is clear from Fig 2 and Fig 4. On the other hand, the application of  $J$  blocks the fluctuations in the occupancy of different Fe-3d orbitals which is clearly seen from the occupation table where a small value of  $J = 0.1$  eV redistributes the electrons among different d-orbitals. A clear orbital selective effect (increase in the occupation of  $d_{yz/xz}$  and  $d_{x^2-y^2}$ ) is seen under the influence of Hund's coupling. Since crystal field splitting is large in FeTe because the value of  $\alpha$  deviates largely from the ideal tetrahedron value unlike the FeSe [45]. It increases the energy difference between the  $d_{x^2-y^2}$  with the  $d_{yz/xz}$  and  $d_{xy}$  orbitals. So Hund's coupling promotes a gradual transfer of electrons from the highly occupied  $d_{x^2-y^2}$  (at  $J = 0.0$  eV) to  $d_{yz/xz}$  and  $d_{xy}$  orbitals with an increase of  $J$  value contrary to FeSe, where a small value of  $J$  is sufficient to transfer the electrons among these orbitals in order to reduce their Coulomb repulsion energy. Thus the different strength of interorbital hybridization and crystal field splitting, which is mainly governed by the anion height, change the occupancy of electrons and band structure of individual Fe-3d orbital. Hund's coupling promotes this differentiation and acts like a band decoupler which was previously studied by Medici *et al.* [46, 47]. This could be the origin of the orbital selective correlation effects seen in iron chalcogenide compounds.

## 4 Conclusion

We presented a systematic study of the effect of Coulomb interaction and Hund's coupling in Fe-3d states in FeSe and FeTe. In both the compounds states around  $E_f$  are predominantly originated from Fe-3d orbital having a pseudogap feature just above the  $E_f$ , whereas hybridized states between Fe-3d and chalcogen-p orbitals lie at higher BE. This hybridization crucially depends on the chalcogen height from the Fe plane and it is weak in case of FeTe where the height of Te anion is higher in comparison to Se anion height in FeSe. Coulomb interaction localizes and shifts the Fe-3d states towards higher BE energy in both the compounds, however this interaction is strongly screened by Te-p bands in FeTe. It is observed that this effect is significant in  $d_{yz/xz}$  and  $d_{x^2-y^2}$  states in case of FeSe. Electrons in these localized states again become itinerant under the influence of  $J$  and a clear orbital selective change is seen in the electronic structure. Similar to  $U$ , Hund's coupling effect is also prominent in FeSe in comparison to FeTe. The

orbital selective nature of the correlation effect is linked to the different values of the interorbital hybridization among different Fe-d orbitals which is mediated via chalcogen-p orbitals. The strength of these interorbital hybridization mainly governs by the geometry of anion tetrahedra, height of anion from the Fe plane ( $z$ ) and anion-Fe-anion angle  $\alpha$ . The difference in the anion tetrahedra geometry turns out to a different orbital selective nature of the correlation effect in both the compounds.

## References

- [1] Wang, Q. Y. *Chin. Phys. Lett.* **29** (2012) 037402.
- [2] J. J. Lee, F. T. Schmitt, R. G. Moore, S. Johnston, Y.-T. Chi, W Li, M. Yi, Z. K. Liu, M. Hashimoto, Y. Zhang, D. H. Lu, T. P. Devereaux, D. -H. Lee and Z.-X Shen *arXiv:1312.2633V5*
- [3] Xu Liu, Def Liu, W. Zhang, J. He, L. Zhao, S. He, D. Mou, F. Li *et al.arXiv:1402.1400v1*
- [4] F.C.Hsu, J.-Y.Luo,K. W.Yeh, T. K. Chen, T. W. Hung, P. M. Wu, Y. C. Lee, Y. L. Huang, Y. Y. Chu, D. C. Yan and M. K. Wu *Natl. Acad. Sci. U.S.A.* **105** (2008) 14262.
- [5] S. Margadonna, Y. Takabayashi, Y. Ohishi, Y. Mizuguchi, Y. Takano, T. Kagayama, T. Nakagawa, M. Takata, and K. Prassides *Phys. Rev. B* **80** (2009) 064506.
- [6] M. Rotter, *Phys. Rev. B* **78** (2008) 020503(R).
- [7] Z. Xu, J. Wen, G. Xu, Q. Jie, Z. Lin, Q. Li, S. Chi, D. K. Singh, G. Gu, and J. M. Tranquada *Phys. Rev. B* **82** (2010) 104525.
- [8] C.Y. Moon, H. J. Choi, *Phys. Rev. Lett.* **104** (2010) 057003.
- [9] F. Ma, W. Ji, J. Hu, Z. Y. Lu, T. Xiang *Phys. Rev. Lett.* **102** (2009) 177003.
- [10] E. Z. Kuchinskii, I. A. Nekrasov, M. V. Sadovski *arXiv:1004.0801v1* (2010)
- [11] and Yoshihiko Takano. *J. Phys. Soc. Jpn.* **78** (2009) 074712.
- [12] S. Li, C. De la Cruz, Q. Huang, Y. Chen, J. W. Lynn, J. Hu, Yi-Lin Huang, Fong-Chi Hsu, Kuo-Wei Yeh, Maw-Kuen Wu and P. Dai *Phys. Rev. B* **79** (2009) 054503.
- [13] Y. Mizugucgi, Y. Hara, K. Deguchi, S. Tsuda, T. Yamaguchi, K. Takeda, H. Kotegawa, H. Tou and Y Takano *Supercond. Sci. Technol.* **23** (2010) 054013.
- [14] M. Bendele, P. Babkevich, S. Katrych, S. N. Gavasaliya, E. Pomjakushina, K. Conder, B. Roessli, A. T. Boothroyd, R. Khasanov and H. Keller *Phys. Rev. B* **82** (2010) 212504.
- [15] R. Viennois, E. Giannini, D. van der Marel, R. cerny *J. Solid State Chemistry* **183** (2010) 769
- [16] K. Nakayama, Y. Miyata, G. N. Phan, T Sato, Y. Tanabe, T. Urata, K. Tanigaki and T. Takahashi *arXiv:1004.0857v1* (2014)
- [17] Markus Aichhorn, Silke Biermann, Takashi Miyake, Antoine Georges and Masatoshi Imada *Phys. Rev. B* **82** (2010) 064504.
- [18] Ansgar Liebsch *Phys. Rev. B* **84** (2011) 180505(R).
- [19] P. Mishra, H. Lohani, R. A. Zargar, V. P. S. Awana and B. R. Sekhar *J. Phys. Condens Matter* **26** (2014) 425501.
- [20] R. Yoshida, T. Wakita, H. Okazaki, Y. Mizuguchi, S. Tsuda, Y. Takano, H. Takeya, K. Hirata, T. Muro, M. Okawa, K. Ishizaka, S. Shin, H. Harima, M. Hirai, Y. Muraoka, and T. Yokoya *J. Phys. Soc. Jpn.* **78** (2009) 034708
- [21] Kazumasa Horigane, Haruhiro Hiraka and Kenji Ohoyama *J. Phys. Soc. Jpn.* **78** (2009) 074718.
- [22] Zargar R A, Pal A, Hafiz A K, Awana V P S *J. Supercond. Nov. Magn.* **27** (2014) 897

- [23] Takashi Miyake, Kazuma Nakamura, Ryotaro Arita and Masatoshi Imada *J. Phys. Soc. Jpn.* **79** (2010) 044705.
- [24] O.K.Andersen, *Phys. Rev. B* **12** (1975) 3060.
- [25] O.K.Andersen and O.Jepsen *Phys. Rev. Lett.* **53** (1984) 2571.
- [26] R. W. Tank, O. Jepsen, A. Burkhardt and O. K. Andersen, *The Stuttgart TB-LMTO-ASA programe,Version 47*
- [27] U. von Barth and L. Hedin, *J. Phys. C*, **4** (1971) 2064.
- [28] Vladimir Anisimov, F. Aryasetiwan and A. I. Lichtenstein *J. Phys. Condens Matter* **9** (1997) 767.
- [29] Giannozzi P et al. <http://www.quantum-espresso.org>.
- [30] G. R. Grechnev, A. S. Panfilov, A. V. Fedorchenko, V.A. Desnenko, I.P. Zhuravleva, S.L. Gnatchenko, D.A. Chareev, O.S. Volkov, A.N. Vasiliev *Ukr. J. Phys.* **57** (2012) 171.
- [31] L. Craco and S. Leoni *EPL* **92** (2010) 67003.
- [32] Y. Xia, D. Qian, L. Wray, D. Hsieh, G.F. Chen, J.L. Luo, N.L. Wang and M.Z. Hasan *Phys. Rev. Lett.* **103** (2009) 037002.
- [33] A. Yamaasaki, Y. Matsui, S.Imada, K. Takase, H. Azuma, T. Muro, Y.Kato, A.Higashiya, A.Sekiyama, S. Suga, M. Yabashi, K.Tamasaku, T. Ishikawa, K. Terashima, H. Kobori, A. Sugimura, N. Umeyama, H. Sato, Y. Hara, N. Miyagawa and S.I. Ikeda *Phys. Rev. B* **82** (2010) 184511.
- [34] L. Craco and M.S. Laad arXiv:1001.3273v1, 2010
- [35] A. Tamai, A.Y. Ganin, E. Rozbicki, J. Bacsa, W. Meevasana, P.D.C. King, M. Caffio, R. Schaub, S. Margadonna, K. Prassides, M.J. Rosseinsky and F. Baumberger *Phys. Rev. Lett.* **104** (2010) 097002.
- [36] Alaska Subedi, Lijun Zhang, D.J. Singh and M.H. Du *Phys. Rev. B* **78** (2008) 134514.
- [37] Fei Chen, Bo Zhou, Yan Zhang, Jia Wei Ou, Jia-Feng Zhao, Cheng He, Qing-Qin Ge, Masashi Arita, Kenya Shimada, Hirofumi Namatame, Masaki Taniguchi, Zhong-Yi Lu, Jiangping Hu, Xiao-Yu Cui and D.L. Feng *Phys. Rev. B* **81** (2010) 014526.
- [38] L. Craco, M.S. Laad and S. Leoni *arXiv:0910.3828v1*, (2009)
- [39] E. Ieki, K. Nakayama, Y. Miyata, T. Sato, H. Miao, N. Xu, X. -P. Wang, P. Zhang, T. Qian, P. Richard, Z. -J. Xu, J. S. Wen, G. D. Gu, H. Q. Luo, H. -H. Wen, H. Ding and T. Takahashi *Phys. Rev. B* **89** (2014) 140506(R).
- [40] H. Miao, P. Richard, Y. Tanaka, K. Nakayama, T. Qian, K. Umezawa, T. Sato, Y.-M. Xu, Y. B. Shi, N. Xu, X.-P. Wang, P. Zhang, H.-B. Yang, Z.-J. Xu, J. S. Wen, G.-D. Gu, X. Dai, J.-P. Hu, T. Takahashi and H. Ding *Phys. Rev. B* **85** (2012) 094506.
- [41] K. Nakayama, T. Sato, P. Richard, T. Kawahara, Y. Sekiba, T. Qian, G. F. Chen, J. L. Luo, N. L. Wang, H.Ding, and T. Takahashi *Phys. Rev. Lett.* **105** (2010) 197001.
- [42] P. Starowicz, H. Schwab, J. Goraus, P. Zajdel, F. Forster, J. R. Rak, M. A. Green, I. Vobornik and F. Reinert *arXiv:1304.7254v1*, (2013)
- [43] Antoine Georges, Luca De' Medici and Jernej Mravlje *arXiv:1207.3033v2*, (2012)
- [44] K Haule and G Kotliar *New Journal of Physics* **11** (2009) 025021
- [45] Z. P. Yin, K. Haule and G. Kotliar *Nature Materials Letters* **10** (2011) 932
- [46] Luca de' Medici *Phys. Rev. B* **83** (2011) 205112.
- [47] Nicola Lanata, Hugo U. R. Strand, Gianluca Giovannetti, Bo Hellsing, Luca de' Medici and Massimo Capone *Phys. Rev. B* **87** (2013) 045122.
- [48] Z. K. Liu, R.-H He, D.H. Lu, M. Yi, Y. L. Chen, M. Hashimoto, R. G. Moore, S.-K. Mo, E. A. Nowadnick, J. Hu, T. J. Liu, Z. Q. Mao, T. P. Devereaux, Z. Hussain and Z.-X. Shen *Phys. Rev. Lett.* **110** (2013) 037003.

Table 1: In this table we have presented the change in the occupancy of electrons in different d orbitals of Iron under the application of different values of U and J in FeSe and FeTe compound.

FeSe					
U(eV)	J(eV)	$d_{xy}$	$d_{xz/yz}$	$d_{3z^2-r^2}$	$d_{x^2-y^2}$
0.0	0.0	1.239	1.300	1.461	1.363
4.0	0.0	0.954	1.581	1.655	0.792
4.0	0.1	1.073	1.257	1.765	1.436
4.0	1.2	1.189	1.203	1.593	1.526
FeTe					
U(eV)	J(eV)	$d_{xy}$	$d_{xz/yz}$	$d_{3z^2-r^2}$	$d_{x^2-y^2}$
0.0	0.0	1.242	1.308	1.462	1.363
3.5	0.0	1.182	1.109	1.569	1.637
3.5	0.1	1.174	1.138	1.558	1.634
3.5	1.2	1.189	1.209	1.514	1.572

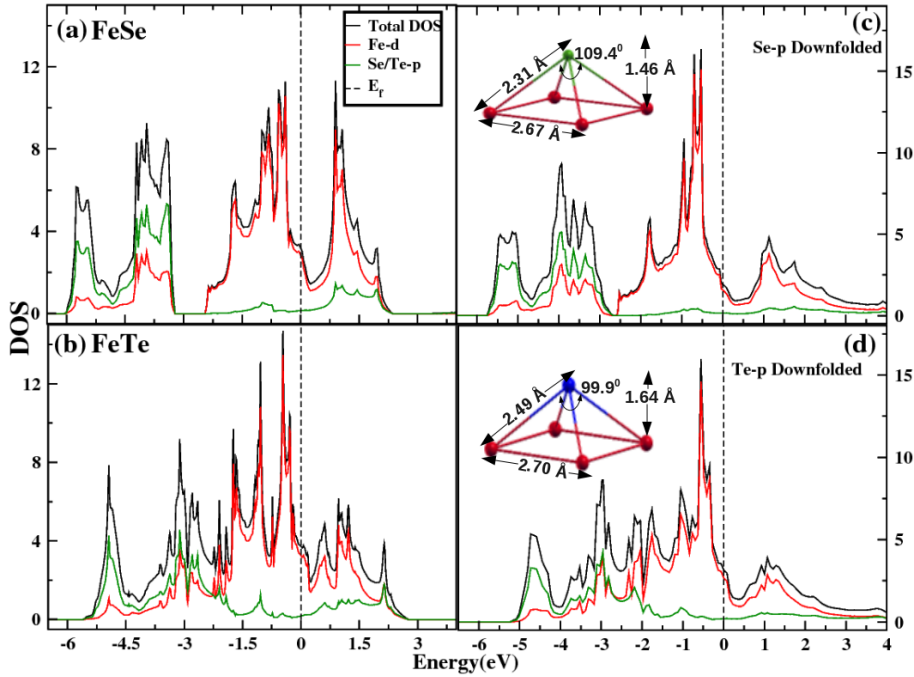


Figure 1: Total and partial DOS have been plotted for FeSe in (a) and for FeTe in (1b). In (c) and (d) total and partial DOS have been calculated, where Se-p and Te-p valence orbitals are doenfolded in FeSe and FeTe respectively. Inset of (c) and (d) shows the anion tetrahedra in FeSe and FeTe respectively. Fe, Se and Te atoms are denoted by red, blue and green clours respectively in the inset pictures (c) and (d).

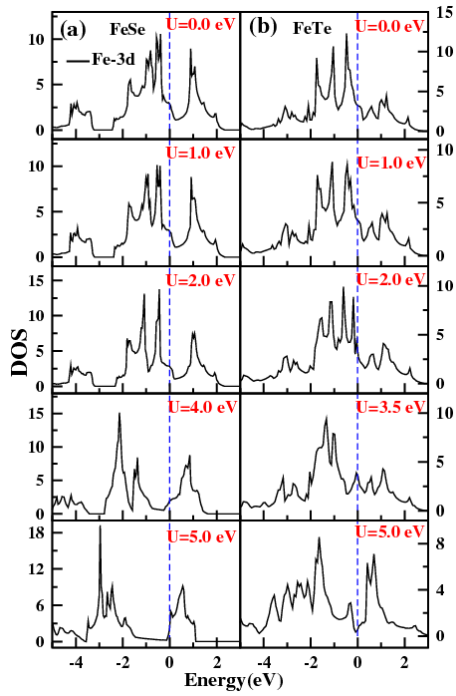


Figure 2: Panel (a) shows changes in Fe-3d states in FeSe at different values of  $U$ , where the value of  $U$  is written in red colour in each plot. Panel (b) shows changes in Fe-3d states in FeTe at different values of  $U$ , where the value of  $U$  is written in red colour in each plot.

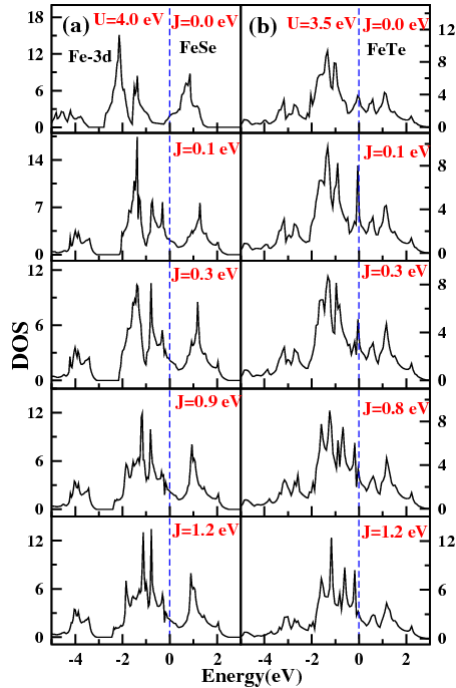


Figure 3: Panel (a) shows changes in Fe-3d states in FeSe at different values of  $J$ , where the value of  $J$  is written in red colour in each plot. Panel (b) shows changes in Fe-3d states in FeTe at different values of  $J$ , where the value of  $J$  is written in red colour in each plot. The value of  $U$  is 4.0 and 3.5 eV in all FeSe and FeTe plots respectively.



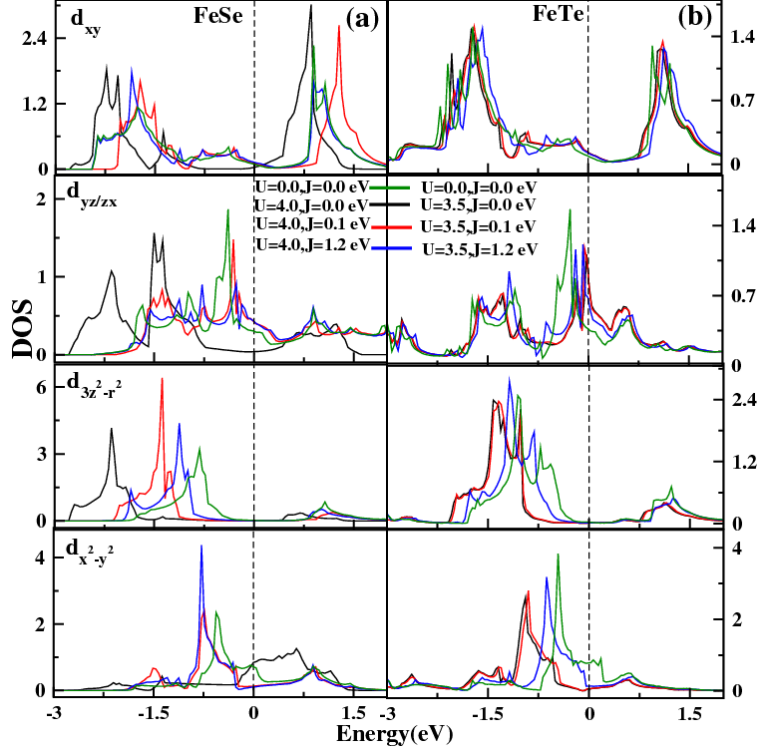


Figure 4: Panel (a) shows changes in the DOS of different d orbitals of Fe atom in FeSe at different values of U and J. Panel (B) shows changes in the DOS of different d orbitals of Fe atom in FeTe at different values of U and J. Different values of U and J are denoted by Green, Black, Red and Blue colours at the top of the Figure.

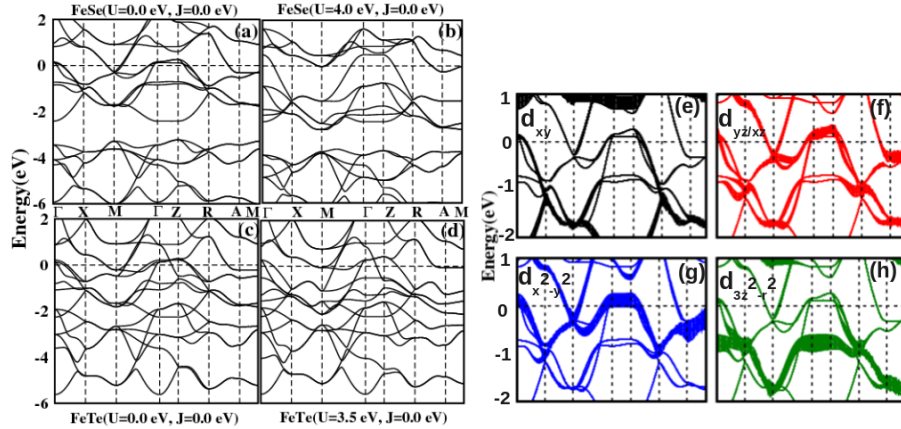


Figure 5: (a) and (b) shows band structure plot of FeSe at  $U = 0.0$  and  $U = 4.0$  eV respectively. (c) and (d) shows band structure plot of FeTe at  $U = 0.0$  and  $U = 3.5$  eV respectively. (e), (f), (g) and (h) shows fatness of bands which are originated from  $d_{xy}$ ,  $d_{yz/xz}$ ,  $d_{x^2-y^2}$  and  $d_{3z^2-r^2}$  respectively for FeSe at  $U$  and  $J = 0.0$  eV.

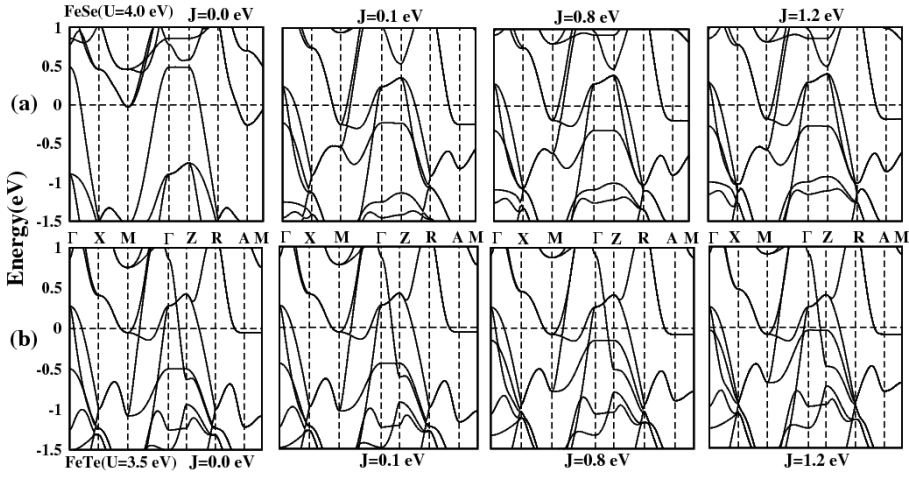


Figure 6: Panel (a) and (b) shows band structure plot for FeSe and FeTe at different values of  $J = 0.0, 0.1, 0.8$  and  $1.2$  eV from left to right respectively. The value of  $U$  is  $4.0$  and  $3.5$  eV in all FeSe and FeTe plots respectively.